ISME

www.nature.com/ismej

ARTICLE

Bacterial volatile organic compounds attenuate pathogen virulence via evolutionary trade-offs

Jianing Wang[1,5], Waseem Raza[1,2,5✉], Gaofei Jiang[1,5], Zhang Yi[1], Bryden Fields[3], Samuel Greenrod[3], Ville-Petri Friman[1,3,4✉], Alexandre Jousset[1], Qirong Shen[1] and Zhong Wei[1✉]

Volatile organic compounds (VOCs) produced by soil bacteria have been shown to exert plant pathogen biocontrol potential owing to their strong antimicrobial activity. While the impact of VOCs on soil microbial ecology is well established, their effect on plant pathogen evolution is yet poorly understood. Here we experimentally investigated how plant-pathogenic *Ralstonia solanacearum* bacterium adapts to VOC-mixture produced by a biocontrol *Bacillus amyloliquefaciens* T-5 bacterium and how these adaptations might affect its virulence. We found that VOC selection led to a clear increase in VOC-tolerance, which was accompanied with cross-tolerance to several antibiotics commonly produced by soil bacteria. The increasing VOC-tolerance led to trade-offs with *R. solanacearum* virulence, resulting in almost complete loss of pathogenicity *in planta*. At the genetic level, these phenotypic changes were associated with parallel mutations in genes encoding lipopolysaccharide O-antigen (*wecA*) and type-4 pilus biosynthesis (*pilM*), which both have been linked with outer membrane permeability to antimicrobials and plant pathogen virulence. Reverse genetic engineering revealed that both mutations were important, with *pilM* having a relatively larger negative effect on the virulence, while *wecA* having a relatively larger effect on increased antimicrobial tolerance. Together, our results suggest that microbial VOCs are important drivers of bacterial evolution and could potentially be used in biocontrol to select for less virulent pathogens via evolutionary trade-offs.

The ISME Journal (2023) 17:443–452; https://doi.org/10.1038/s41396-023-01356-6

INTRODUCTION

Microbial volatile organic compounds (VOCs) are a broad group of low molecular weight lipophilic gaseous compounds that are produced as the result of primary and secondary metabolism, often having bioactive functions [1]. VOCs can have several ecological effects, ranging from cell-to-cell communication to plant growth stimulation and activation of systematic plant resistance in response to biotic and abiotic stresses [2]. Moreover, microbial VOCs often have high antimicrobial activity that inhibit bacterial growth, increasing the competitiveness of VOC-producers [3, 4]. As bacterial species vary in their innate sensitivity [5], VOCs could drive changes in the composition and diversity of microbial communities via ecological sorting [6]. Moreover, VOC-selection could potentially increase the proportion of VOC-tolerant bacterial genotypes through positive selection. Yet, no data exists on the long-term effects of VOC selection on bacterial tolerance and resistance evolution.

Unlike antibiotics, molecular targets and potential resistance mechanisms to VOCs are yet to be discovered. Short-term VOC-exposure has previously been reported to lead to degradation of the cell envelope and fragmentation of cytoplasmic contents with plant pathogenic *Clavibacter michiganensis* bacterium [7] and *Monilinia laxa* phytopathogenic fungi [8]. Moreover, VOCs have been reported to stimulate DNA alkylation, affect DNA repair and metabolic processes [9], and induce protein expression related to ABC transporter system and potential detoxification of VOCs [3, 4]. It is thus possible that changes in genes governing these cell processes might provide resistance or tolerance to VOCs. Similar to other antimicrobials, evolving resistance to VOCs could be costly, leading to trade-offs with other traits linked with bacterial competitive ability or virulence [10, 11]. In support of this, it has been shown that exposing phytopathogenic *Ralstonia solanacearum* bacterium to VOCs produced by *Bacillus amyloliquefaciens* leads to reduced growth and expression of several virulence factors, including biofilm formation, motility and root colonization [4, 12]. Another recent study showed that VOC exposure led to a wide range of hyphal abnormalities and downregulation of genes associated with sporulation yield and conidial maturation in *Alternaria solani* fungal pathogen [13]. While these changes were likely caused by altered gene expression due to the short length of the experiments, it is possible that prolonged VOC selection could lead to heritable genetic changes in VOC-tolerance and its associated costs.

Here, we used experimental evolution to directly test (i) if long-term exposure to VOCs selects for increased tolerance; (ii) if

[1]Jiangsu Provincial Key Lab for Organic Solid Waste Utilization, National Engineering Research Center for Organic-based Fertilizers, Jiangsu Collaborative Innovation Center for Solid Organic Waste Resource Utilization, Nanjing Agricultural University, Weigang 1, Nanjing 210095, PR China. [2]Institute for Environmental Biology, Ecology & Biodiversity, Utrecht University, Padualaan 8, 3584 CH Utrecht, The Netherlands. [3]Department of Biology, University of York, Wentworth Way, York YO10 5DD, UK. [4]Department of Microbiology, University of Helsinki, Helsinki 00014, Finland. [5]These authors contributed equally: Jianing Wang, Waseem Raza, Gaofei Jiang. ✉email: waseem@njau.edu.cn; ville-petri.friman@helsinki.fi; weizhong@njau.edu.cn

Received: 2 August 2022 Revised: 21 December 2022 Accepted: 4 January 2023
Published online: 12 January 2023

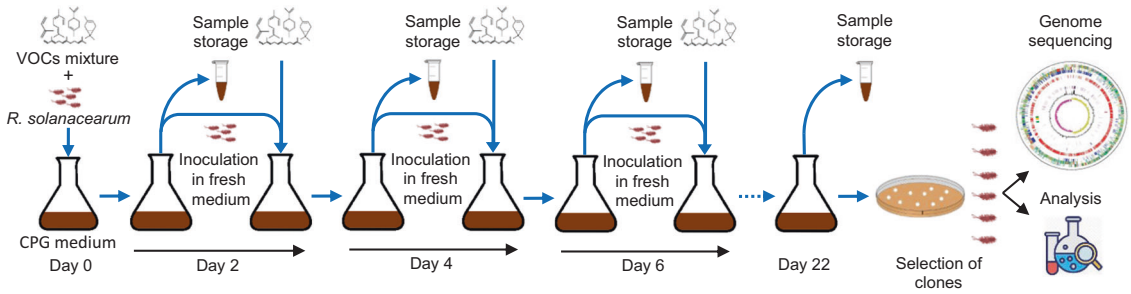

Fig. 1 Schematic representation of the experimental design, where plant pathogenic *Ralstonia solanacearum* was evolved in the absence and presence of three VOC mixture concentrations in sealed flasks for 22 days with two-day serial transfers. Subsamples were stored at every transfer and final samples were used to select for evolved clones and quantify changes in *R. solanacearum* tolerance and virulence, and for sequencing to identify parallel mutations shared between treatment replicates.

VOC-tolerance correlates with pathogen resistance to antibiotics and virulence in vitro and *in planta*; and (iii) to determine genetic changes underlying these phenotypic changes. To achieve this, we exposed phytopathogenic *R. solanacearum* bacterium to three concentrations of a synthetic mixture of 25 VOCs produced by *B. amyloliquefaciens* T-5 biocontrol bacterium (Supplementary Table S1; refs. [4, 14]) for 22 days (≈550*R. solanacearum* generations; 11 serial transfers; Fig. 1). *R. solanacearum* was chosen as the model pathogen species due to its global importance for agriculture as a causal agent of bacterial wilt disease, wide host range and broad geographic distribution [14]. Moreover, as no effective control methods exists, the importance of antimicrobial VOCs as a potential biocontrol strategy against *R. solanacearum* should be evaluated. One such potential VOC-producing biocontrol bacterium could be *B. amyloliquefaciens* T-5, which is known to produce a range of different VOCs [3] and shown to be able to limit bacterial wilt of tomato in greenhouse experiments [15]. In this experiment, we evaluated if these biocontrol effects might vanish over time due to the evolution of VOC tolerance by *R. solanacearum* by correlating changes in *R. solanacearum* VOC-tolerance with changes in antibiotic resistance and virulence. Moreover, the potential underlying mutations were determined using whole-genome sequencing at the end of the experiment, and the significance of two candidate mutations was independently confirmed using reverse genetic engineering.

MATERIALS AND METHODS

Bacterial strains and growth conditions

We used the bacterial pathogen *Ralstonia solanacearum* strain QL-Rs1115 (China General Microbiology Culture Collection Center, accession No. 9487) as our target pathogen that was isolated from the roots of a wilted tomato plant [16]. *R. solanacearum* was stored at −80 °C in casamino acid-peptone-glucose (CPG) medium (1 g casamino acid, 10 g peptone, 5 g glucose and pH 7.0) containing 70% glycerol [17]. During the experiments, *R. solanacearum* was grown on CPG agar plates and liquid CPG media unless stated otherwise. The *Escherichia coli* strains DH5α and S17-1 were used for plasmid construction and conjugational transfer, respectively. They were grown at 37 °C in LB medium (10 g tryptone, 10 g NaCl, 5 g yeast extract; pH 7.0) with shaking (180 rpm) or on LB agar plate (supplemented with 1.5% agar).

Evolution experiment setup

For the in vitro evolution experiment, a single colony of ancestral *R. solanacearum* strain was pre-grown in CPG medium for 24 hours at 30 °C with shaking (170 rpm). Later, the cells of *R. solanacearum* were washed and suspended in 0.85% NaCl (~10^7 CFU/ml) and inoculated (25 µl) in 25 ml of fresh CPG medium in 100 ml Erlenmeyer flasks (N = 24). Flasks were incubated at 30 °C with shaking (170 rpm) for 2 hours before they were evenly assigned to four treatments with six replicates: no VOC (No-VOC), low (L-VOC), intermediate (I-VOC) and high (H-VOC) VOC treatments, with final VOC concentrations corresponding to 0 ppm, 0.5 ppm, 1 ppm and 2 ppm of VOC mixture, respectively. The VOC mixture was prepared by mixing 25 individual VOC compounds in the same ratio as they are produced by *B. amyloliquefaciens* T-5 bacterium after 3 days of growth in the soil [3], which was tested to inhibit *R. solanacearum* growth by 30% in one-on-one plate assay (Supplementary Table S1; ref. [4]). While most of VOCs were available in liquid form, some solid VOCs had to be dissolved in methanol, where µg VOC = µl methanol. Methanol was previously confirmed to not have any effect on the growth or virulence of *R. solanacearum* [3, 4, 12, 18]. Similarly, the three VOC mixture concentrations (low, intermediate and high) were determined based on their antimicrobial effects in liquid CPG media, resulting in 15%, 30% and 55% growth inhibition of *R. solanacearum*, respectively (Supplementary Fig. S1). During the selection experiment, all flasks were sealed with Parafilm and incubated at 30 °C with shaking (170 rpm) after initial inoculation and addition of VOCs. Serial transfers took place after two days of growth by transferring 25 µl of thoroughly homogenized liquid culture from the old flasks (0.1% of the total population) into fresh flasks containing 25 ml of CPG medium supplemented with VOC mixture corresponding with the concentrations of given treatments. Serial transfers were continued for 22 days (11 transfers) and subsamples (10 ml) were cryopreserved at −80 °C every second transfer (in 30% of glycerol) for growth and virulence trait assays and genome sequencing, which were performed later (Fig. 1).

Determining *R. solanacearum* population densities during the VOC selection experiment

To determine changes in *R. solanacearum* population densities during the selection experiment, 1 ml liquid culture collected at each time point (2 days each) as described above was diluted by 500 times and spread on CPG agar plates. The plates were incubated at 30 °C and viable cell counts as CFU/ml were determined after two days of incubation.

Selection of evolved *R. solanacearum* clones at the end of the selection experiment

To characterize evolutionary changes driven by VOC-selection, we randomly isolated three *R. solanacearum* clones per replicate population from all six replicate selection lines of two treatments (18 clones per treatment): *R. solanacearum* evolved in the absence of VOCs (No-VOC) and in the high VOC concentration (H-VOC). Only the H-VOC treatment was chosen for evolutionary measurements due to large number of measurements and because the negative effect of VOC mixture, and hence the strength of selection, was the highest in this treatment. In addition, three clones of the ancestral strain were used for all measurements to establish baseline for the strain's initial performance. All *R. solanacearum* samples stored at −80 °C were thawed on ice for 15 minutes, diluted by 500 times with sterilized water and spread on CPG agar plates. After two days of incubation at 30 °C, three clones for each treatment replicate were randomly selected, regrown in liquid CPG medium and cryopreserved on 96-well plates to characterize evolutionary changes at the phenotypic and genotypic levels relative to ancestor in following assays.

VOC-tolerance assay

The tolerance of *R. solanacearum* ancestor and evolved No-VOC and H-VOC clones were evaluated by re-exposing them to the VOC mixture and five individual VOCs present in the mixture in separate assays. Five selected individual VOCs that showed antimicrobial activity included nonanone, undecanal, oleic acid, heptadecane and benzothiazole, which belonged to five distinct chemical classes: ketones, aldehydes, fatty acids, alkanes and

benzenes, respectively. The VOC tolerance assay was conducted both in liquid CPG media (exposure via liquid) and using agar plate assays (exposure through air). In liquid media assays, conditions were kept the same as in the selection experiment, using 100 ml Erlenmeyer flasks containing 25 ml CPG medium, which were inoculated with *R. solanacearum* cell cultures and subsequently exposed to VOCs (mixture and individual compounds) at three concentration levels (0.5 ppm, 1 ppm and 2 ppm). After two days of growth, 1 ml liquid culture was collected from each flask, diluted by 500 times, and spread on CPG agar plates to determine viable cell counts (CFU/ml) as described earlier.

In agar media assays, divided Petri plates with CPG agar medium (15 g/l agar) were used for the VOC tolerance assay as follows. One-half of the Petri plate was inoculated with two drops (5 µl each) of *R. solanacearum* cell suspensions (~10^7 CFU/ml) at 4 cm apart. Petri plates were then incubated at 30 °C for 12 h to initiate bacterial growth after sterile Whatman filter paper discs (~10 mm diameter) supplemented with VOCs were placed on other halves of the Petri plates. VOC treatments with three concentration levels (12.5 µl, 25 µl and 50 µl) of VOC mixture and five individual VOCs were used to compare the tolerance of ancestor, No-VOC and H-VOC clones. Petri plates were sealed with Parafilm and incubated for further two days at 30 °C. Also, sterile filter paper discs inoculated with nothing were used as a negative control. Later, *R. solanacearum* colonies were removed along with agar medium using a sterilized scalpel and CFU/ml were determined as described previously. In both VOC tolerance assays; every clone was measured in triplicate and the VOC effects were calculated as the percentage increase or decrease compared to when clones were grown in the absence of VOCs in the negative control treatment.

Antibiotic-tolerance assay

The cross-tolerance of *R. solanacearum* ancestor and evolved No-VOC and H-VOC clones were measured against three antibiotics with distinct molecular targets: polymyxin B sulfate (bacterial cell membrane), erythromycin (50S subunit rRNA) and rifamycin (RNA polymerase). Three different concentrations of antibiotics (determined in preliminary experiments) were used along with no-antibiotic negative control: 75, 150 and 300 µg/ml for polymyxin B sulfate, 2.5, 5, 10 µg/ml for erythromycin and 0.25, 0.5 and 0.75 µg/ml for rifamycin. Antibiotics were mixed with CPG medium at different concentrations and then 195 µl was added into the wells of 96-well microtiter plates. Later, 5 µl overnight culture suspensions (10^7 CFU/ml) of all clones were added and plates were incubated at 30 °C with shaking (170 rpm) for two days. Every clone was measured in triplicate and the experiment was repeated twice. The antibiotic effects were determined as the percentage increase or decrease compared to when clones were grown in the absence of antibiotics.

Growth curve assay

The growth curves for all clones were measured using 96-well microtiter plates. A single colony of the ancestor, No-VOC and H-VOC clones were pre-grown in CPG medium at 30 °C with 170 rpm shaking overnight. The liquid cultures were then washed with sterilized water, adjusted to 10^7 CFU/ml and 5 µl was added into the wells of microtiter plates containing 195 µl of CPG medium. Bacterial growth was measured as a change in optical density (OD_{600}) after 4, 8, 12, 18, 24, 30, 36, 48 and 60 h of incubation at 30 °C with 170 rpm shaking. The growth rate, maximum biomass, area under the growth curve, doubling time and lag-phase time were determined from this data using the R package Growthcurver 0.3.1 [19], which fits a basic form of the logistic equation common in ecology and evolution to experimentally-obtained growth curve data. The logistic equation gives the number of cells N_t at time t.

$$N_t = K/1 + (K - N_0/N_0)e^{-rt}$$

Here, the population size at the beginning of the growth curve is given by N_0. The maximum possible population size in a particular environment, or the carrying capacity, is given by K. The growth rate was reported as intrinsic growth rate of the population (r) per hour (h^{-1}). Every clone was measured in triplicate and the experiment was repeated twice.

Virulence trait assays in vitro

The quantified virulence traits included motility, antioxidant potential, extracellular polysaccharides and biofilm formation. Before virulence traits assays, the overnight liquid culture of *R. solanacearum* clones was washed and suspended in 0.85% NaCl (10^7 CFU/ml). Both swarming and swimming motility were determined on CPG agar plates at 30 °C containing 0.7% and 0.3% (w/v) agar, respectively. The zone of migration was measured in four directions after three days for swarming motility and after two days for swimming motility [4, 5]. To evaluate the antioxidant potential of *R. solanacearum* clones, catalase and superoxide dismutase (SOD) activities were determined. The catalase activity was determined according to the method of Chance and Maehly [20] and defined as the amount of H_2O_2 (µM) broken down per minute by one milligram of protein under the assay conditions. The SOD activity was determined using the nitroblue tetrazolium (NBT) method [21]. The amount of SOD enzyme that inhibited 50% of NBT reduction was defined as one enzyme unit (U). For the extracellular polysaccharides production assay, liquid culture samples of *R. solanacearum* were inoculated (20 µl) in fresh CPG medium. After three days of growth at 30 °C, extracellular polysaccharides were precipitated using ice-cold ethanol and quantified by the phenol-sulfuric acid method as described in previous reports [4, 22]. For biofilm formation assay, 96-well microtiter plates were used and biofilm formation was determined after three days of incubation at 30 °C. Crystal violet staining and biofilm estimation was performed as described previously [23]. Every clone was measured in triplicate and the experiment was repeated twice. The data for virulence traits was calculated as an increase or decrease in trait values relative to the ancestor.

Virulence measured *in planta*

Seeds of tomato *cv*. Hezuo 903 were surface sterilized using $NaOCl_4$ (5%) and grown on wet (sterile H_2O) Whatman paper for three days at 30 °C. The germinated seeds were dipped overnight in water-washed cell cultures (10^8 CFU/ml) of *R. solanacearum* ancestor and evolved No-VOC and H-VOC clones separately and then three seedlings were transferred to each pot (15 × 8 cm) containing vermiculite and peat mixture (1:1). The seedlings were grown until the germination of the third true leaf and then thinned to one plant per pot. The pots were placed in a growth chamber (25 °C temperature, 12 h light, 12 h dark, 65–80% relative humidity). Meanwhile, the ancestor, No-VOC and H-VOC *R. solanacearum* clones were grown in CPG medium overnight at 30 °C and washed and suspended in sterilized water (10^8 CFU/ml). To ensure high infectivity, 50 ml of the cell cultures of *R. solanacearum* clones were added to each pot and pots were watered with ½ strength Murashige and Skoog medium every second day [24]. Each clone had six replicates and the disease index was calculated after four weeks [16] as follows: the plants were scored on a scale of 0–4, where 0 = no wilted leaf, 1 ≤ 25% wilted leaves, 2 = 25–50% wilted leaves, 3 = 50–75% wilted leaves and 4 ≥75% wilted leaves or dead plant. The disease index was calculated using the following equation:

$$\text{Disease index} = \left[\frac{\Sigma(\text{number of diseased plants} \times \text{disease score})/}{(\text{total number of plants investigated} \times \text{highest disease score})}\right].$$

Genome sequencing and variant calling analysis

To identify the genotypic changes and their relationship with the phenotypic response of *R. solanacearum* clones, genomic DNA were extracted from three ancestral and 18 evolved clones from both No-VOC and H-VOC treatments to produce draft genomes for variant calling analysis. The DNA was extracted using DNeasy Kit (QIAGEN) according to the manufacturer's instructions. Genomic DNA was quantified using TBS-380 fluorometer (Turner BioSystems Inc., Sunnyvale, CA) and at least 1 µg of high-quality genomic DNA ($OD_{260/280}$ = 1.8~2.0, >6 µg) were used to construct sequencing libraries for paired-end sequencing. Paired-end libraries with insert sizes of ~400 bp were prepared following Illumina's standard genomic DNA library preparation procedure. Purified genomic DNA was sheared into smaller fragments with the desired size by Covaris and blunt ends were generated by using T4 DNA polymerase. After adding an 'A' base to the 3′ end of the blunt phosphorylated DNA fragments, adapters were ligated to the ends of the DNA fragments. The desired fragments were purified through gel-electrophoresis, then selectively enriched and amplified by PCR. The index tag was introduced into the adapter at the PCR stage as appropriate and a library-quality test was performed. The qualified paired-end library was used for HiSeq sequencing (Illumina, PE150 mode). Genome sequencing was performed by Shanghai Biozeron Biotechnology Co., Ltd (Shanghai, China).

Raw reads for each sample were quality-checked with FastQC (v.0.11.4) [25]. Samples identified to have read files containing an observable percentage of Illumina adapter contamination were removed using cutadapt (v.2.3) [26]. Raw reads for each sample were assembled into contigs *de novo* with SPAdes (v. 3.14.0) using the isolate mode [27]. Variants for ancestor, No-VOC and H-VOC clones (18 clones for each; 3 per

replicate) were identified by mapping reads to PacBio reference of *R. solanacearum* strain RS-N (NCBI accession no. CP099579-CP099581) using Snippy (v.4.6.0; https://github.com/tseemann/snippy). A GenBank file was created with gene annotations using PROKKA (v.1.14.5; Kingdom: Bacteria, Genus: Ralstonia) for the snippy to assign gene information to identified variants [28]. BLASTp was utilized to identify the protein functions of identified hypothetical proteins. Genetic differences identified in the ancestral strain relative to the RS-N reference strain were not considered in downstream analyses as these were present already prior to the start of the selection experiment. Identified variants were grouped by treatment and given running number from 1 to 3 within each replicate population. Prophages were identified in strain *de novo* assemblies using the PHASTER web server (https://phaster.ca/) which automatically classified them into intact (score > 90), questionable (score 70–90) and incomplete (score < 70) prophages based on their size and the presence of phage-like and phage cornerstone genes [29]. Insertion sequence (IS) movement was determined using previously described method [30]. Briefly, IS were identified in the ancestral strain using ISEScan v.1.7.2.3 [31] and were clustered with Mash [32]. Their taxonomic identities were determined through comparisons with ISFinder database (https://isfinder.biotoul.fr/). IS movement in experimental clones was determined using ISMapper v.2.0.2 [33].

Construction of single mutant strains for linking parallel SNPs with bacterial phenotypes

To verify the effect of parallel SNPs on bacterial phenotypes, we constructed single mutant strains carrying in-frame deletion in either *pilM* or *wecA* gene as descripted previously [34]. The *R. solanacearum* clone used in the reverse-genetics experiment was the same ancestral *R. solanacearum* strain QL-Rs1115 used for the evolution experiment. To construct a complete in-frame deletion of *pilM* or *wecA* genes, the ~500-bp border arms A (upstream) and B (downstream) of each gene were separately amplified by PCR using pilM-A1F/-A2R or wecA-A1F/-A2R and pilM-B1F/-B2R or wecA-B1F/-B2R primer pairs, respectively (Table S2). The reverse primer A2R for the upstream, and forward primer B1F for the downstream, contained 15 bases of aligning nucleotides that were fully complementary. Later, the two purified border fragments of each gene were subjected to a second round of PCR amplification using pilM-A1F/B2R or wecA-A1F/B2R primer pairs to overlap two border arms into a ~ 1-kb DNA fragment. This overlapped fragment was purified using agarose gel, ligated into the *EcoR V* predigested pBluescript II KS+ and transferred to *E. coli* DH5α (Table S3). Later, the plasmid was extracted, and cloned into the *BamHI* and *Hind III* digested pK18mobsacB [35] and transferred into *E. coli* S17-1 (Table S3). The resulting pK18pilM and pK18wecA plasmids were separately transferred from *E. coli* S17-1 into ancestral *R. solanacearum* by natural conjugation and positively selected on sucrose medium. The deletion of *pilM* and *wecA* at its original location of ancestral *R. solanacearum* was confirmed by 1-kb reduction of the colony PCR products using primers pilM-A1F/B2R or wecA-A1R/B2F. The mutant strains were named *ΔpilM* and *ΔwecA*. A similar recombination procedure was used to complement *ΔpilM* and *ΔwecA* with point-mutated *pilM* and *wecA* genes. Briefly, 965-bp and 1305-bp upstream and 1277-bp and 799-bp downstream fragments of *pilM* and *wecA* genes were amplified using primer pairs pilM-F1/-R1ovlP or wecA-F1/-R1ovlP and pilM-mutP/-R2 or wecA-mutP/-R2, respectively. The forward primers of downstream fragments, pilM-mutP or wecA-mutP, contained both overlapping sequences (inverse complementary sequence of pilM-R2ovlP and wecA-R2ovlP, respectively) and point mutation sequences: insertion of C to replace T at the position of 462 in *wecA* gene and insertion of G to replace GC at the position of 825 in *pilM* gene. The purified border fragments of each gene were subjected to a second round of PCR amplification using the primer pairs pilM-F1/-R2 or wecA-F1/-R2 to overlap two border arms into a ~2-kb DNA fragments. These DNA products were cloned into pBluescript II KS+, sequences validated and then cloned into pK18mobsacB for parental conjunction experiments as described above. The complementation of point mutated *pilM* and *wecA* genes was confirmed by 2-kb increase of colony PCR products using primers pilM-F1/-R2 or wecA-F1/-R2 after positive selection on sucrose medium. The point mutants were named as $\Delta pilM^{iG}$ and $\Delta wecA^{iC}$, respectively, and their phenotypes characterized regarding growth, VOC and antibiotic tolerances (only the highest concentration), virulence traits (swarming and swimming motility, biofilm formation and EPS production) and virulence *in planta* as described earlier.

Statistical analysis

For the experimental evolution selection experiment, repeated measures generalized linear model (GLMs) were used to account for temporal autocorrelation and pseudoreplication in time. Here, the growth of *R. solanacearum* was considered as the response variable, which was explained by VOC treatment that had four different levels: three VOC mixture concentrations and no-VOC control treatment. Separate GLMs were conducted to evaluate evolutionary changes after the selection experiment for a subset of evolved clones that were randomly isolated from No-VOC and H-VOC treatments. Here, a factorial GLM analysis was used to explain variation in VOC tolerance of No-VOC and H-VOC treatment clones relative to ancestral strain by VOC type (six levels: VOC mixture and five individual VOCs), VOC concentration (three levels: low, intermediate and high) and evolutionary history (three levels: ancestor, No-VOC and H-VOC) as fixed independent variables. The final model included all main effects and two- and three-way interactions. Similar factorial GLM analyses were conducted to explain variation in antibiotic tolerance of ancestral and No-VOC and H-VOC treatment clones. To evaluate growth and virulence trait differences between No-VOC and H-VOC treatment clones, one-way ANOVA was used. To visualize the overall differences among ancestor, No-VOC and H-VOC treatment clones based on growth and virulence traits, principal component analysis (PCA) was used after trait data standardization (subtracting the mean trait value with the minimum observed value of that trait and then dividing by the difference between the maximum and minimum observed values for that trait). In addition, permutational multivariate analysis of variance (PERMANOVA) was conducted to evaluate if the centroids of distance matrices differed between ancestor, No-VOC and H-VOC clone treatment groups based on 9999 permutations and Bray-Curtis dissimilarity matrix using PAST 4.0.3 software [36]. The rest of the above-mentioned statistical analysis was performed using SPSS version 19.0 statistical software (SPSS, Inc., Chicago, IL, USA).

RESULTS AND DISCUSSION

VOC exposure reduces *R. solanacearum* population densities and selects for increased VOC tolerance

The *R. solanacearum* population densities were clearly reduced by VOC exposure, with higher concentrations having more severe effects (Fig. 2; Supplementary Table S4). The VOC effects stabilized after the first 8 days of the selection experiment, which could be indicative of *R. solanacearum* adaptation to VOCs due to rapid emergence of resistance mutations. To study this, we isolated three *R. solanacearum* clones per replicate population from all six No-VOC and H-VOC treatment replicates (18 clones per treatment) at the end of the experiment. In addition, three ancestral strain clones were used to establish baseline comparison. Evolutionary

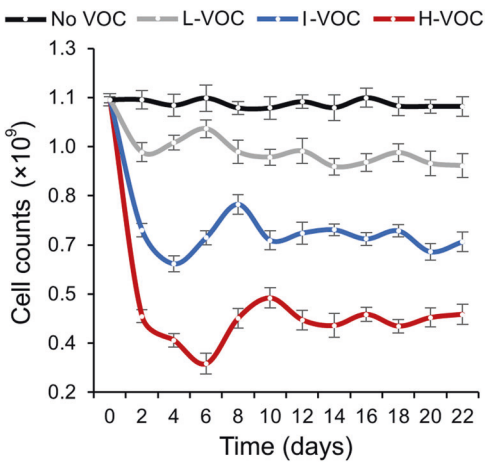

Fig. 2 Population density dynamics of plant pathogenic *Ralstonia solanacearum* in the absence and presence of three concentrations of volatile organic compound (VOC) mixture. *Ralstonia solanacearum* was evolved in the absence (No-VOC) and presence of low (L-VOC), intermediate (I-VOC) and high (H-VOC) VOC concentrations in sealed flasks for 22 days with two-day serial transfers. Subsamples were stored at every transfer and used to determine population densities as cell counts per ml.

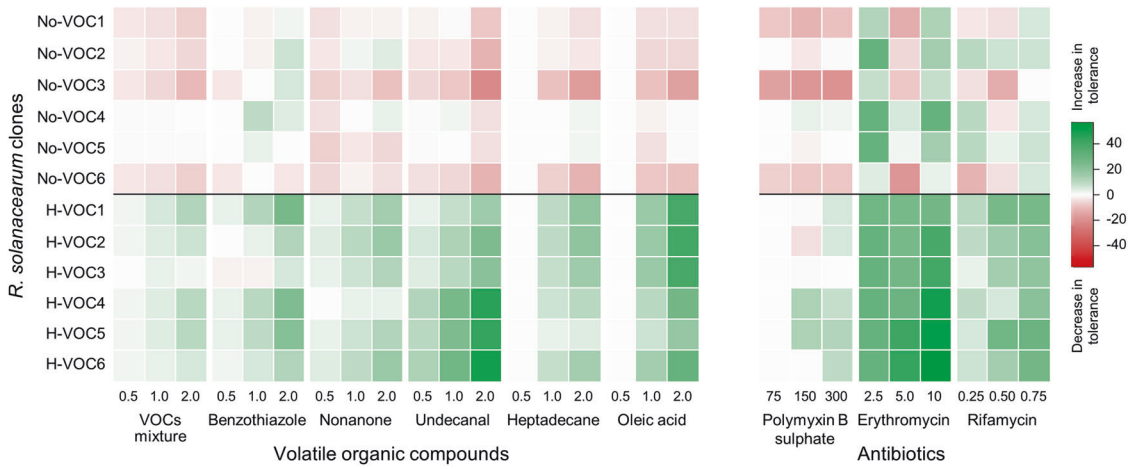

Fig. 3 Selection by volatile organic compounds (VOCs) leads to increased tolerance to both VOCs and antibiotics. Comparison of VOC (left) and antibiotic (right) tolerances of control (No-VOC) and high VOC (H-VOC) replicate selection lines relative (%) to the ancestor in the presence of VOC mixture, five antimicrobial VOC constituents (benzothiazole, nonanone, undecanal, heptadecane and oleic acid) and three antibiotics (polymyxin B sulfate, erythromycin and rifamycin). Each square represents the mean of three replicate clones isolated from the final time point and three measurement concentrations of VOCs (ppm) and antibiotics (μg/ml) were used. Green and red colors represent increases and decreases in tolerance relative (%) to the ancestor clones, respectively.

changes in VOC-tolerance were quantified both in liquid (direct contact) and agar culture media (indirect contact via air) by re-exposing all clones to the VOC-mixture and five individual antimicrobial VOCs present in the mixture (Supplementary Table S1). We found that evolved H-VOC clones showed increased VOC-tolerance relative to the ancestral and No-VOC clones and this difference was greater when measured at higher VOC concentrations (Liquid media assay; Fig. 3, Supplementary Figs. S2, S3 and Supplementary Table S5). While all clones showed 15–20% lower growth inhibition on agar medium compared to liquid culture, the overall patterns of inhibition were similar between the two methods ($R^2 = 0.96$, $p < 0.0001$). Moreover, evolved H-VOC clones were more tolerant to individual VOCs compared to VOC-mixture, showing the highest tolerance to undecanal followed by oleic acid, benzothiazole, heptadecane and nonanone. In contrast, evolved No-VOC clones remained equally susceptible to individual VOCs compared to ancestral clones, and even in some cases showed concentration-dependent increase in susceptibility to nonanone (0.5 ppm), undecanal (0.5 and 2.0 ppm) and oleic acid in liquid media (1.0 and 2.0 ppm; Fig. 3).

As it is well known that exposure to one stress can select for cross-tolerance to other stresses [37], we quantified the tolerance of evolved *R. solanacearum* clones to three antibiotics with distinct molecular targets: polymyxin B sulfate (bacterial cell membrane), erythromycin (50 s subunit rRNA) and rifamycin (RNA polymerase). Overall, evolved H-VOC clones showed improved tolerance to all antibiotics relative to the ancestral clones and this difference was greater when measured at higher antibiotic concentrations (Fig. 3; Supplementary Fig. S4 and Supplementary Table S6). While *R. solanacearum* showed innate resistance to polymyxin B sulfate, the H-VOC clones evolved the highest level of tolerance to erythromycin followed by rifamycin (Fig. 3). Overall, No-VOC clones remained equally susceptible to antibiotics as ancestral clones, except for showing improved tolerance to erythromycin. Furthermore, the VOC and antibiotic tolerances were positively correlated at all measured concentrations (Fig. S5), even though the magnitude varied between different compounds and used concentrations (Supplementary Tables S5 and S6). Together, these results demonstrate that VOC-mixture can select for increased, generalized tolerance to several different VOCs and antibiotics with different modes of action. Overall, these results are in line with previous work where the evolution of antibiotic resistance has been shown to correlate positively with other toxic compounds, such as herbicides [38, 39] and plant allelochemicals [40], indicating that bacteria might employ general stress response strategies to cope with a variety of antimicrobials.

VOC tolerance leads to trade-off with *R. solanacearum* growth and virulence

To explore the evolution of potential trade-offs, changes in VOC-tolerance were correlated with changes in evolved *R. solanacearum* clones' growth and virulence measured in vitro and *in planta*. Both H-VOC and No-VOC clones showed an increase in maximum biomass and area under the growth curve and reduced lag-phase relative to the ancestral clones (Fig. 4a), which suggests that *R. solanacearum* adapted to the growth media as has been reported previously in another study [40]. However, evolved H-VOC clones showed lower growth rates and increased lag-phases relative to No-VOC clones, indicative of a growth cost (*e.g.*, due to potential resource allocation trade-off) associated with VOC-tolerance (Fig. 4a; Supplementary Figs. S6, S7). Such costs could partly explain why H-VOC populations could not restore their growth and population densities during the selection experiment despite evolving more tolerant to VOCs. Moreover, H-VOC clones showed a clear reduction in several virulence traits relative to ancestral and No-VOC clones, including swarming motility, superoxide dismutase activity, biofilm formation and extracellular polysaccharides production, while four H-VOC clones showed an increase in swimming motility relative to ancestral clones. Additionally, all virulence traits correlated positively with each other but negatively with most of the growth traits, except for growth rate and lag-phase time (Fig. 5a; Supplementary Fig. S9), indicative of trade-off between growth and virulence as shown previously [41]. In contrast, the virulence traits of evolved No-VOC clones did not differ from the ancestral clones, except for showing a slight increase in swimming motility (Fig. 4b; Supplementary Fig. S8). A clear separation between treatments was also observed using principal component analysis based on all phenotypic traits (*PERMANOVA*, $F_{(2,\ 38)} = 4.41$, $P = 0.009$), where H-VOC clones formed a distinct cluster from No-VOC clones and ancestral clones, while No-VOC clones did not significantly differ from the ancestral clones, except for five clones from 3 replicates that showed a clear reduction in virulence traits. While more research is needed to understand phenotypic variation emerging

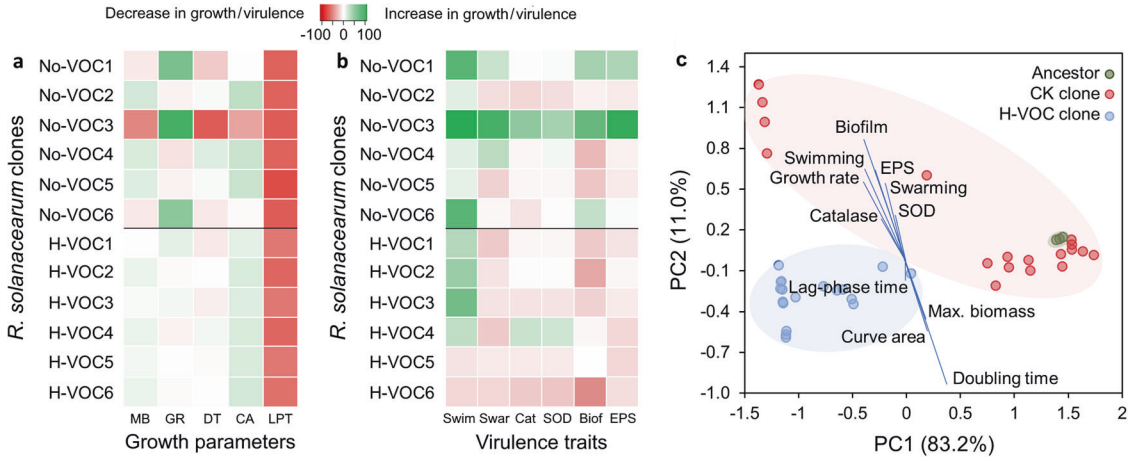

Fig. 4 Evolution of volatile organic compound (VOC)-tolerance leads to trade-off with *Ralstonia solanacearum* virulence. a Comparison of growth traits [maximum biomass (MB), growth rate (GR), doubling time (DT), growth curve area (CA) and lag-phase time (LPT)] between evolved control (No-VOC) and high VOC (H-VOC) replicate selection lines relative (%) to the ancestor. **b** Comparison of virulence traits [swimming motility (Swim), swarming motility (Swar), catalase activity (Cat), superoxide dismutase activity (SOD), biofilm formation (Biof) and extracellular polysaccharides production (EPS)] between evolved No-VOC and H-VOC replicate selection lines relative (%) to the ancestor. In (**a**) and (**b**), each square represents the mean of three replicate clones isolated from the final time point, while green and red colors represent the increase and decrease in trait values relative (%) to the ancestor, respectively. **c** Principal component analysis based on all growth and virulence traits of ancestor and evolved No-VOC and H-VOC replicate selection lines. Each data point in (**c**) represents one replicate clone.

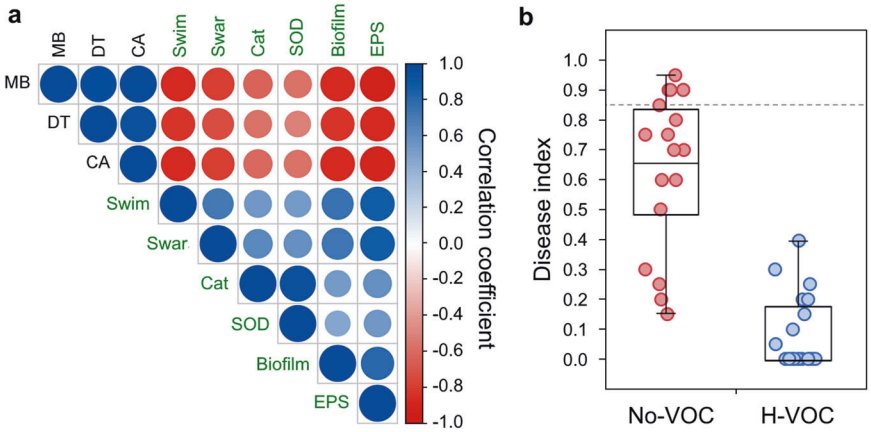

Fig. 5 Evolution of volatile organic compounds (VOC)-tolerance leads to trade-off with *Ralstonia solanacearum* virulence. a Pearson correlations of growth traits [maximum biomass (MB), doubling time (DT) and growth curve area (CA)] and virulence traits [swimming motility (Swim), swarming motility (Swar), catalase activity (Cat), superoxide dismutase activity (SOD) and extracellular polysaccharides production (EPS)] of evolved *Ralstonia solanacearum* clones derived from high VOC (H-VOC) treatment at the end of the selection experiment. Positive correlations are displayed in blue and negative correlations in red color. The color intensity and the size of the circles are proportional to the value of correlation coefficients. **b** Comparison of disease index (DI) between evolved control (No-VOC) and H-VOC treatment replicate selection lines relative to the ancestor (dotted line) *in planta*. Each data point in (b) represents one replicate clone.

in No-VOC treatment, one likely explanation could be adaptation to the growth media and conditions during the experiment (Fig. 4c; Supplementary Table S7).

Changes in *R. solanacearum* virulence were also quantified *in planta* using root colonization assay. A clear reduction in *R. solanacearum* virulence was found with evolved H-VOC clones relative to No-VOC and the ancestral clones. Interestingly, No-VOC clones also showed a slight reduction in virulence, but this effect was much stronger with H-VOC clones (Fig. 5b). Together, these results suggest that microbial VOCs can select for more tolerant but less virulent plant pathogen genotypes, which is in line with previous research, where increases in antimicrobial resistance have often been associated with reduced fitness [42], competitive ability [43], growth rate [44] and virulence [45].

Genetic basis of VOC-tolerance and reduced virulence

To understand the genetic basis of VOC-tolerance, and associated trait correlations, we sequenced all phenotyped clones from No-VOC and H-VOC treatments. The sequenced clones acquired only a few mutations (1.3 and 2.4 mutations per clone in No-VOC and H-VOC treatments, respectively), which included intergenic mutations and small deletions with No-VOC clones and missense mutations and small insertions and deletions with H-VOC clones (Fig. 6a). Most mutations were located in the chromosome (12 loci) and only a few mutations were found in the megaplasmid of H-VOC clones (*R. solanacearum* has a bi-partite genome [46]). Importantly, most mutations were nonsynonymous with H-VOC clones (66–72% of sequenced clones), including highly parallel missense mutations in the glycosyl transferase gene (*wecA*) and frameshift mutations in fimbrial type-4 assembly protein-encoding gene (*pilM*). Moreover, a few clones had missense mutations in type IV pilus secretin gene (*pilQ*), staphyloferrin B siderophore synthase gene (*sbnC*), transcriptional regulator gene (*pehR*) and flagellar hook-length control protein-encoding gene (*fliK*) (Fig. 6b; Supplementary Table S8). Our phenotypic results suggest that VOC-tolerance was likely driven by some type of generalized

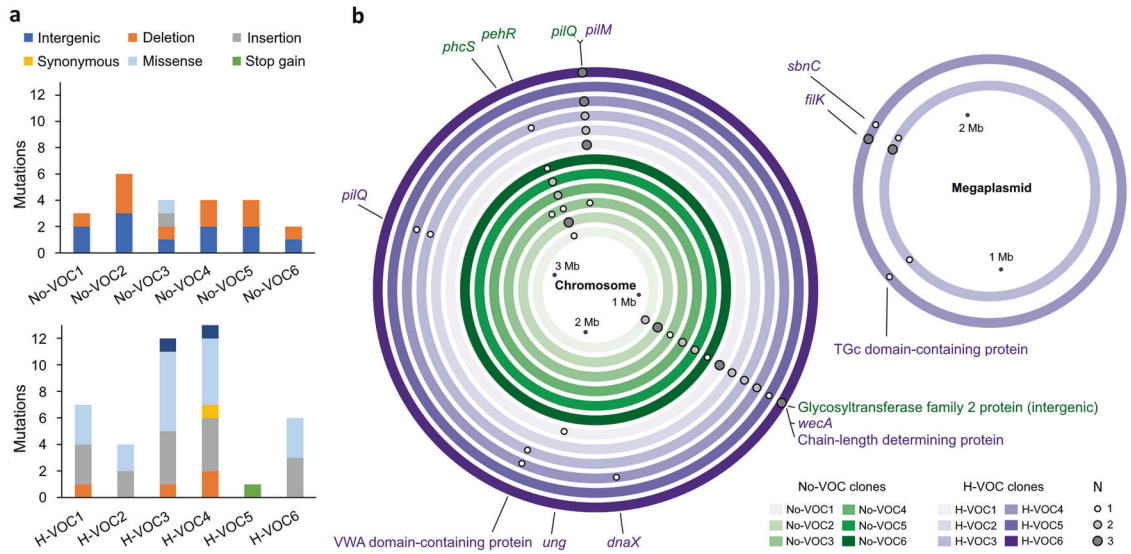

Fig. 6 Volatile organic compounds (VOC)-tolerance is linked to parallel mutations in lipopolysaccharide and type-IV pilus encoding genes. a The number of different types of mutations found in control (No-VOC) and high VOC (H-VOC) treatment replicates. Each bar represents the number of mutations of three clones per replicate selection line and different colors represent different types of mutations. **b** The observed mutations across different loci on the chromosome (large circles) and the megaplasmid (small circles) of No-VOC (green) and H-VOC clones (purple). Large circles denote different treatment replicates, and small grey dots and their size indicate the loci and number of clones with given mutations, respectively. The closely located variants are grouped and labeled with the name of the gene in which those are identified. The gene names are colored by their treatment: No-VOC clones with green and H-VOC clones with purple. Mutations in the megaplasmid were only observed in two H-VOC treatment replicates.

resistance mechanism that provided tolerance to several types of VOCs and antibiotics (Fig. S5). The *wecA* gene is important for bacterial outer membrane structure via lipopolysaccharides (LPS) O-antigen biosynthesis [47] and LPS is known to form a permeation barrier against the entry of several antibiotics [48], providing tolerance, especially against hydrophobic antibiotics such as erythromycin and rifamycin [49]. Most VOCs are also nonpolar, hydrophobic compounds [1] and can cause modifications in cell membrane fluidity and permeability, allowing their entry into the cell [50]. Moreover, parallel mutations were observed in genes encoding pilus (*pilM*) and flagella (*fliK*; only with a few clones) that form an important part of the bacterial outer membrane and have previously been associated with antibiotic resistance [49, 51]. While the exact mechanisms of LPS and pilus mutations on antimicrobial resistance are not yet properly understood, they both were recently found to confer resistance to colistin in *Pseudomonas aeruginosa* [52]. High parallelism of *wecA* and *pilM* mutations in the H-VOC treatment thus suggests that these mutations were important for the evolution of generalized tolerance, potentially via reduced outer membrane permeability to hydrophobic VOCs and antibiotics. Crucially, both *wecA* and *pilM* are also important for bacterial virulence by affecting adhesion, colonization, biofilm formation, motility and pathogenesis [53–56]. Mutations in these genes thus also likely explain the observed reduction in virulence of H-VOC clones.

Two parallel mutations were also found in evolved No-VOC clones (61% of sequenced clones). The first one was a disruptive in-frame deletion in transcription regulator (*pehR*), which has been linked with swimming and twitching motility [57], potentially explaining changes in swimming motility in No-VOC clones. The second point mutation was observed in the 1254230-intergenic region upstream to *wecA* (737 bp), which unlikely affected the expression of *wecA* due to tRNA region between. Furthermore, one clone from No-VOC treatment (CK3) had mutations in *pilQ* (fimbrial assembly) and *phcS* (histidine kinase; quorum-sensing) genes. While these mutations were not associated with increased VOC-tolerance, they could explain the slightly reduced virulence of No-VOC clones [58, 59].

We also explored if VOC-exposure triggered the movement of insertion sequences (IS) or prophages, which could have contributed to observed phenotypic adaptations [60]. Overall, a greater IS gain and loss was found in four regions of H-VOC clone genomes. However, this IS movement occurred in intergenic regions, making it difficult to predict their phenotypic effects (Supplementary Fig. S10). Similarly, while ten prophages could be identified, no prophage loss or movement was observed (Supplementary Table S9). Together, these findings suggest that only a few mutations in pilus and LPS genes were required for a clear increase in VOC-tolerance, that had clear pleiotropic effects in terms of reduced virulence in vitro and *in planta*.

Genetically engineered *pilM* and *wecA* mutants show increased VOC and antibiotic tolerances but reduced virulence

To validate the contribution of *pilM* and *wecA* mutations for observed bacterial phenotypes, reverse genetic engineering was used to construct single mutant strains for both genes in the ancestral strain background (see methods). Overall, both $\Delta pilM^{iG}$ and $\Delta wecA^{iC}$ mutants showed changes in their antimicrobial tolerances and virulence, though their individual contributions were lower than H-VOC clones. While the growth curves of $\Delta pilM^{iG}$ and $\Delta wecA^{iC}$ did not differ from the ancestral strain (Supplementary Fig. S11), they showed higher VOC tolerance to the mixture and five individual VOCs, with $\Delta wecA^{iC}$ being overall more tolerant (9–40%) than $\Delta pilM^{iG}$ (6–21%; Fig. 7). In the case of antibiotic tolerance, $\Delta pilM^{iG}$ showed 5–8% higher tolerance to all three antibiotics compared to ancestral strain, while $\Delta wecA^{iC}$ showed complete resistance to polymyxin B sulfate, clear increase in tolerance to rifamycin (36%) and slightly increased tolerance to erythromycin (4%) compared to ancestral strain (Fig. 7). Regarding the virulence traits measured in vitro, $\Delta pilM^{iG}$ showed reduction only in swimming motility while $\Delta wecA^{iC}$ showed reduction in both swimming and swarming motility (Fig. 8). Moreover, while both mutants showed reduced virulence *in planta* relative to the ancestral strain, this effect was much stronger with $\Delta pilM^{iG}$ (58% reduction) compared to $\Delta wecA^{iC}$ (32% reduction; Fig. 8). These results suggest that both *pilM* and *wecA* mutations that were

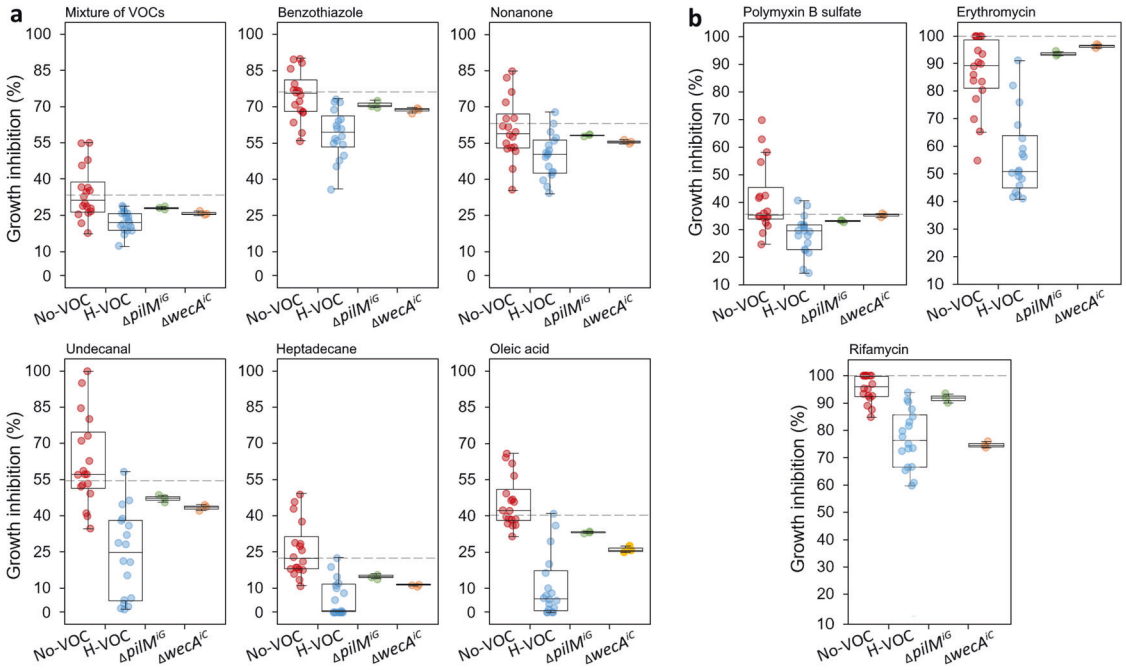

Fig. 7 Comparison of tolerance of evolved clones and Δ*pilM*^{iG} and Δ*wecA*^{iC} mutants to volatile organic compounds (VOC) and antibiotics. The inhibitory effect of VOC mixture and five individual antimicrobial VOCs (**a**) and three antibiotics (**b**) on the growth of evolved clones and Δ*pilM*^{iG} and Δ*wecA*^{iC} mutants. The evolved clones were derived from control (No-VOC) and high level of VOC (H-VOC) treatments at the end of the selection experiment. Exposure to VOCs was done in divided Petri plates on solid CPG agar media at the highest VOC measurement concentration (50 µl) used in the selection experiment, and for antibiotics, the highest measurement concentrations of 300 µg/ml for polymyxin B sulfate, 10 µg/ml for erythromycin and 0.75 µg/ml for rifamycin were used. The growth inhibition was quantified as percentage reduction relative to when the same clones and point mutants were grown in the absence of VOCs or antibiotics after two days of growth. In all panels, 'No-VOC' and 'H-VOC' denote clones that evolved in the absence and presence of VOCs, respectively, and the dotted grey line shows the growth inhibition of the ancestral clone. Three clones per treatment replicate were used and each data point represents one replicate clone.

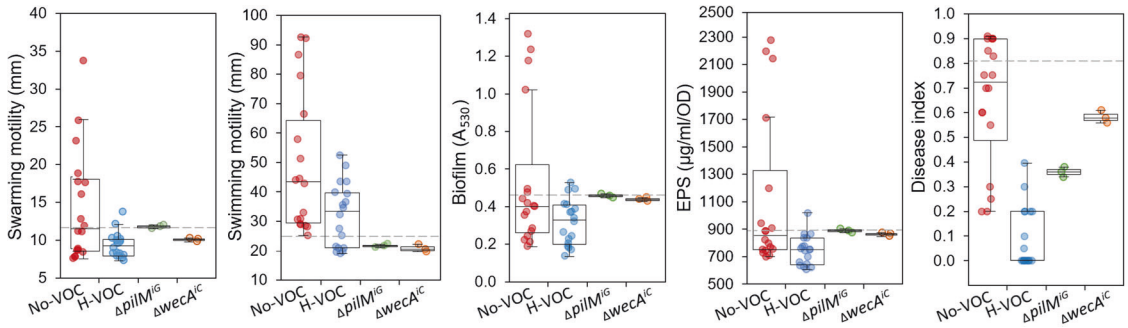

Fig. 8 Comparison of virulence traits in vitro and *in planta* (disease index) of evolved clones and Δ*pilM*^{iG} and Δ*wecA*^{iC} mutants. The evolved clones were derived from control (No-VOC) and high level of volatile organic compound (H-VOC) treatments at the end of the selection experiment. The dotted grey line shows the virulence traits of the ancestral clone. Three clones per treatment replicate were used and each data point represents one replicate clone. Note: for SNPs validation experiment, antioxidant activity (superoxide dismutase and catalase) was not included as it was found similar among ancestral, No-VOC and H-VOC clones. EPS extracellular polysaccharides.

observed to evolve in parallel under VOC selection affected both increased antimicrobial tolerance and reduced virulence, potentially having synergistic, epistatic effects with H-VOC clones.

Our results show that in addition to shaping microbial ecology [2], microbial VOCs can also drive plant pathogen evolution by selecting VOC-tolerant mutants that show cross-tolerance to several antibiotics. Mechanistically, VOC-tolerance was likely driven by reduced membrane permeability, which could have provided tolerance to both hydrophobic antibiotics and VOCs used in our experiments. The mutations associated with tolerance were also linked to reduced virulence in vitro and *in planta*. VOCs could thus be used as selective agents to weaken plant pathogen virulence via fitness trade-offs, similar to trade-offs exerted by parasitic bacteriophages [18, 61]. In the future, it would be interesting to explore if more specialized VOC-tolerance might evolve when bacteria are exposed to single VOCs instead of complex VOC mixtures. However, considering the high prevalence and complexity of VOCs in the soils [62], microbial VOCs could commonly select for generalized stress tolerance mechanisms instead of narrower specialist tolerance. Also, further long-term selection experiments are required to explore if *R. solanacearum* can evolve compensatory mutations [63] that will help it regain virulence subsequently after evolving VOC-tolerance. Additional experiments in soil and plant mesocosms are also required to quantify potential VOC-tolerance evolution in spatially structured and more complex microbial communities [64, 65] that could for

example magnify the costs of adaptation [66]. In conclusion, our findings suggest that antimicrobial tolerance in plant pathogens can evolve through VOC exposure by another bacterium, highlighting the importance of community context for the evolution of antibiotic resistance in natural environments [67].

DATA AVAILABILITY

The genome sequences of ancestral, No-VOC and H-VOC clones of *Ralstonia solanacearum* QL-Rs1115 are available at NCBI Sequence Read Archive (SRA) under the accession number SAMN29421919. The rest of the data are available in the article and its online supplementary material.

REFERENCES

1. Schulz-Bohm K, Gerards S, Hundscheid M, Melenhorst J, de Boer W, Garbeva P. Calling from distance: attraction of soil bacteria by plant root volatiles. ISME J. 2018;12:1252–62.
2. Garbeva P, Weisskopf L. Airborne medicine: bacterial volatiles and their influence on plant health. N Phytol. 2020;226:32–43.
3. Raza W, Wang J, Wu Y, Ling N, Wei Z, Huang Q, et al. Effects of volatile organic compounds produced by *Bacillus amyloliquefaciens* on the growth and virulence traits of tomato bacterial wilt pathogen *Ralstonia solanacearum*. Appl Microbiol Biotechnol. 2016;100:7639–50.
4. Raza W, Ling N, Liu D, Wei Z, Huang Q, Shen Q. Volatile organic compounds produced by *Pseudomonas fluorescens* WR-1 restrict the growth and virulence traits of *Ralstonia solanacearum*. Microbiol Res. 2016;192:103–13.
5. Tyc O, Zweers H, de Boer W, Garbeva P. Volatiles in inter-specific bacterial interactions. Front Microbiol. 2015;6:1412.
6. Yuan J, Zhao M, Li R, Huang Q, Raza W, Rensing C, et al. Microbial volatile compounds alter the soil microbial community. Environ Sci Pollut Res. 2017;24:22485–93.
7. Rajer FU, Wu H, Xie Y, Xie S, Raza W, Tahir HAS, et al. Volatile organic compounds produced by a soil-isolate, *Bacillus subtilis* FA26 induce adverse ultra-structural changes to the cells of *Clavibacter michiganensis* ssp. *sepedonicus*, the causal agent of bacterial ring rot of potato. Microbiology. 2017;163:523–30.
8. Toral L, Rodríguez M, Martínez-Checa F, Montaño A, Cortés-Delgado A, Smolinska A, et al. Identification of volatile organic compounds in extremophilic bacteria and their effective use in biocontrol of postharvest fungal phytopathogens. Front Microbiol. 2021;12:773092.
9. Alpha CJ, Campos M, Jacobs-Wagner C, Strobel SA. Mycofumigation by the volatile organic compound-producing fungus *Muscodor albus* induces bacterial cell death through DNA damage. Appl Environm Microbiol. 2015;81:1147–56.
10. Melnyk AH, Wong A, Kassen R. The fitness costs of antibiotic resistance mutations. Evol Appl. 2015;8:273–83.
11. Basra P, Alsaadi A, Bernal-Astrain G, O'Sullivan ML, Hazlett B, Clarke LM, et al. Fitness tradeoffs of antibiotic resistance in extraintestinal pathogenic *Escherichia coli*. Genome Biol Evol. 2018;10:667–79.
12. Raza W, Ling N, Yang L, Huang Q, Shen Q. Response of tomato wilt pathogen *Ralstonia solanacearum* to the volatile organic compounds produced by a biocontrol strain *Bacillus amyloliquefaciens* SQR-9. Sci Rep. 2016c;6:24856.
13. Zhang D, Qiang R, Zhao J, Zhang J, Cheng J, Zhao D, et al. Mechanism of a volatile organic compound (6-methyl-2-heptanone) emitted from *Bacillus subtilis* ZD01 against *Alternaria solani* in potato. Front Microbiol. 2022;12:808337.
14. Jiang G, Wei Z, Xu J, Chen H, Zhang Y, She X, et al. Bacterial wilt in China: history, current status, and future perspectives. Front Plant Sci. 2017;8:1549.
15. Tan S, Dong Y, Liao H, Huang J, Song S, Xu Y, et al. Antagonistic bacterium *Bacillus amyloliquefaciens* induces resistance and controls the bacterial wilt of tomato. Pest Manag Sci. 2013;69:1245–52.
16. Wei Z, Yang XM, Yin SX, Shen Q, Ran W, Xu Y. Efficacy of *Bacillus*-fortified organic fertiliser in controlling bacterial wilt of tomato in the field. Appl Soil Ecol. 2011;48:152–9.
17. Kelman A. The relationship of pathogenicity in *Pseudomonas solanacearum* to colony appearance on a tetrazolium medium. Phytopathology. 1954;44:693–5.
18. Gurney J, Brown SP, Kaltz O, Hochberg ME. Steering phages to combat bacterial pathogens. Trends Microbiol. 2020;28:85–94.
19. Sprouffske K, Wagner A. Growthcurver: an R package for obtaining interpretable metrics from microbial growth curves. BMC Bioinform. 2016;17:172.
20. Chance B, Maehly AC. Assay of catalase and peroxidases. Methods Enzymol. 1955;2:764–75.
21. Zhou Z, White KA, Polissi A, Georgopoulos C, Raetz CR. Function of *Escherichia coli* MsbA, an essential ABC family transporter, in lipid A and phospholipid biosynthesis. J Biol Chem. 1998;273:12466–75.
22. Dubois M, Gilles KA, Hamilton JK, Rebers PA, Smith F. Colorimetric method for determination of sugars and related substances. Analy Chem. 1956;28:350–6.
23. O'Toole GA, Kolter R. Initiation of biofilm formation in *Pseudomonas fluorescens*WCS365 proceeds via multiple, convergent signalling pathways: a genetic analysis. Mol Microbiol. 1998;28:449–61.
24. Murashige T, Skoog F. A revised medium for rapid growth and bio assays with tobacco tissue cultures. Plant Physiol. 1962;15:473–97.
25. Andrews S. FastQC: A quality control tool for high throughput sequence data. 2020. http://www.bioinformatics.babraham.ac.uk/projects/fastqc/
26. Martin M. Cutadapt removes adapter sequences from high-throughput sequencing reads. EMBnet J. 2011;17:10–12.
27. Sarovich DS, Price EP. SPANDx: a genomics pipeline for comparative analysis of large haploid whole genome re-sequencing datasets. BMC Res Notes. 2014;7:618.
28. Seemann T Prokka: rapid prokaryotic genome annotation. Bioinformatics. 30:2068–9.
29. Arndt D, Grant JR, Marcu A, Sajed T, Pon A, Liang Y, et al. PHASTER: a better, faster version of the PHAST phage search tool. Nucleic Acids Res. 2016;44:W16–W21.
30. Greenrod STE, Stoycheva M, Elphinstone J, Friman VP. Genetically related *Ralstonia solanacearum* phytopathogenic bacteria carry similar insertion sequences. BioRxv. 2022. https://doi.org/10.1101/2022.07.16.500299
31. Xie Z, Tang H. ISEScan: automated identification of insertion sequence elements in prokaryotic genomes. Bioinformatics. 2017;33:3340–7.
32. Ondov BD, Treangen TJ, Melsted P, Mallonee AB, Bergman NH, Koren S, et al. Mash: fast genome and metagenome distance estimation using MinHash. Genome Biol. 2016;17:132.
33. Hawkey J, Hamidian M, Wick RR, Edwards DJ, Billman-Jacobe H, Hall RM, et al. ISMapper: identifying transposase insertion sites in bacterial genomes from short read sequence data. BMC Genom. 2015;16:667.
34. Zhang Y, Luo F, Wu D, Hikichi Y, Kiba A, Igarashi Y, et al. *PrhN*, a putative *marR* family transcriptional regulator, is involved in positive regulation of type III secretion system and full virulence of *Ralstonia solanacearum*. Front Microbiol. 2015;6:357.
35. Schäfer A, Tauch A, Jäger W, Kalinowski J, Thierbach G, Pühler A. Small mobilizable multi-purpose cloning vectors derived from the *Escherichia coli* plasmids pK18 and pK19: selection of defined deletions in the chromosome of *Corynebacterium glutamicum*. Gene 1994;145:69–73.
36. Hammer Ø, Harper DA, Ryan PD. PAST: paleontological statistical software package for education and data analysis. Palaeontol Electron. 2001;4:1–9.
37. van Overbeek LS, Eberl L, Givskov M, Molin S, van Elsas JD. Survival of, and induced stress resistance in, carbon-starved *Pseudomonas fluorescence* cells residing in soil. Appl Environ Microbiol. 1995;61:4202–8.
38. Liao H, Li X, Yang Q, Bai Y, Cui P, Wen C, et al. Herbicide selection promotes antibiotic resistance in soil microbiomes. Mol Biol Evol. 2021;38:2337–50.
39. Barbosa da Costa N, Hébert MP, Fugère V, Terrat Y, Fussmann GF, Gonzalez A, et al. A glyphosate-based herbicide cross-selects for antibiotic resistance genes in bacterioplankton communities. mSystems 2022;7:e0148221.
40. Alderley CL, Greenrod STE, Friman VP. Plant pathogenic bacterium can rapidly evolve tolerance to an antimicrobial plant allelochemical. Evol Appl. 2021;15:735–50.
41. Perrier A, Peyraud R, Rengel D, Barlet X, Lucasson E, Gouzy J, et al. Enhanced in planta fitness through adaptive mutations in *EfpR*, a dual regulator of virulence and metabolic functions in the plant pathogen *Ralstonia solanacearum*. PLoS Pathog. 2016;12:e1006044.
42. Wang X, Wei Z, Li M, Wang X, Shan A, Mei X, et al. Parasites and competitors suppress bacterial pathogen synergistically due to evolutionary trade-offs. Evolution. 2017;71:733–46.
43. Vogwill T, MacLean RC. The genetic basis of the fitness costs of antimicrobial resistance: a meta-analysis approach. Evol Appl. 2015;8:284–95.
44. Bagel S, Hüllen V, Wiedemann B, Heisig P. Impact of *gyrA* and *parC* mutations on quinolone resistance, doubling time, and supercoiling degree of *Escherichia coli*. Antimicrob Agents Chemother. 1999;434:868–75.
45. Olivares J, Alvarez-Ortega C, Linares JF, Rojo F, Köhler T, Martínez JL. Overproduction of the multidrug efflux pump MexEF-OprN does not impair *Pseudomonas aeruginosa* fitness in competition tests, but produces specific changes in bacterial regulatory networks. Environ Microbiol. 2012;148:1968–81.
46. Salanoubat M, Genin S, Artiguenave F, Gouzy J, Mangenot S, Arlat M, et al. Genome sequence of the plant pathogen *Ralstonia solanacearum*. Nature. 2002;415:497–502.
47. Lehrer J, Vigeant KA, Tatar LD, Valvano MA. Functional characterization and membrane topology of *Escherichia coli* WecA, a sugar-phosphate transferase initiating the biosynthesis of enterobacterial common antigen and O-antigen lipopolysaccharide. J Bacteriol. 2007;189:2618–28.
48. Delcour AH. Outer membrane permeability and antibiotic resistance. BBA. 2009;1794:808–16.
49. Wang J, Ma W, Fang Y, Liang H, Yang H, Wang Y, et al. Core oligosaccharide portion of lipopolysaccharide plays important roles in multiple antibiotic resistance in *Escherichia coli*. Antimicrob Agents Chemother. 2021;65:e00341–21.

50. Trombetta D, Castelli F, Sarpietro MG, Venuti V, Cristani M, Daniele C, et al. Mechanisms of antibacterial action of three monoterpenes. Antimicrob Agents Chemother. 2005;49:2474–8.
51. Nandi S, Swanson S, Tomberg J, Nicholas RA. Diffusion of antibiotics through the PilQ secretin in Neisseria gonorrhoeae occurs through the immature, sodium dodecyl sulfate-labile form. J Bacteriol. 2015;197:1308–21.
52. O'Brien TJ, Figueroa W, Welch M. Decreased efficacy of antimicrobial agents in a polymicrobial environment. ISME J. 2022;16:1694–704.
53. Karuppiah V, Derrick JP. Structure of the PilM-PilN inner membrane type IV pilus biogenesis complex from *Thermus thermophilus*. J Biol Chem. 2011;286:24434–42.
54. Gilbreath JJ, Colvocoresses Dodds J, Rick PD, Soloski MJ, Merrell DS. Enterobacterial common antigen mutants of *Salmonella enterica* serovar *Typhimurium* establish a persistent infection and provide protection against subsequent lethal challenge. Infect Immun. 2012;80:441–50.
55. Jurcisek J, Greiner L, Watanabe H, Zaleski A, Apicella MA, Bakaletz LO. Role of sialic acid and complex carbohydrate biosynthesis in biofilm formation by nontypeable *Haemophilus influenzae* in the chinchilla middle ear. Infect Immun. 2005;73:3210–8.
56. Shi W, Sun H. Type IV pilus-dependent motility and its possible role in bacterial pathogenesis. Infect Immun. 2002;70:1–4.
57. Allen C, Gay J, Simon-Buela L. A regulatory locus, *pehSR*, controls polygalacturonase production and other virulence functions in Ralstonia solanacearum. Mol Plant Microbe Interact. 1997;10:1054–64.
58. Narulita E, Addy HS, Kawasaki T, Fujie M, Yamada T. The involvement of the PilQ secretin of type IV pili in phage infection in *Ralstonia solanacearum*. Biochem Biophys Res Commun. 2016;469:868–72.
59. Clough SJ, Lee KE, Schell MA, Denny TP. A two-component system in *Ralstonia* (*Pseudomonas*) *solanacearum* modulates production of PhcA-regulated virulence factors in response to 3-hydroxypalmitic acid methyl ester. J Bacteriol. 1997;179:3639–48.
60. Razavi M, Kristiansson E, Flach CF, Larsson DGJ. The association between insertion sequences and antibiotic resistance genes. mSphere. 2020;5:e00418–20.
61. Wang X, Wei Z, Yang K, Wang JN, Jousset A, Xu YC, et al. Phage combination therapies for bacterial wilt disease in tomato. Nat Biotechnol. 2019;37:1513–20.
62. Raza W, Mei X, Wei Z, Ling N, Yuan J, Wang J, et al. Profiling of soil volatile organic compounds after long-term application of inorganic, organic and organic-inorganic mixed fertilizers and their effect on plant growth. Sci Total Environ. 2017;607-608:326–38.
63. Loftie-Eaton W, Bashford K, Quinn H, Dong K, Millstein J, Hunter S, et al. Compensatory mutations improve general permissiveness to antibiotic resistance plasmids. Nat Ecol Evol. 2017;1:1354–63.
64. Raza W, Wei Z, Jousset A, Qirong S, Friman VP. Extended plant metarhizobiome: understanding volatile organic compound signaling in plant-microbe metapopulation networks. mSystems. 2021;6:e00849–21.
65. Raza W, Wang J, Jousset A, Friman VP, Wang S, Wei Z, et al. Bacterial community richness shifts the balance between volatile organic compound-mediated microbe–pathogen and microbe–plant interactions. Proc R Soc B. 2020;287:20200403.
66. Alseth EO, Pursey E, Luján AM, McLeod I, Rollie C, Westra ER. Bacterial biodiversity drives the evolution of CRISPR-based phage resistance. Nature. 2019;574:549–52.
67. Bottery MJ, Pitchford JW, Friman VP. Ecology and evolution of antimicrobial resistance in bacterial communities. ISME J. 2021;15:939–48.

ACKNOWLEDGEMENTS

This work was supported by the National Natural Science Foundation of China (Nos. 42090064, 42090062, 42007038, 31972504, 32170180, 42277113, 41922053) to ZW, GJ and QS, and the National Key Research and Development Program of China (No. 2018YFD1000800), the European Union's Horizon 2020 research and innovation programme under the Marie Skłodowska-Curie grant agreement (No. 838710-ReproDev to WR), the Royal Society (No. RSG\R1\180213 and No. CHL\R1\180031 to VPF) and jointly by a grant from UKRI, Defra, and the Scottish Government, under the Strategic Priorities Fund Plant Bacterial Diseases Programme (No. BB/T010606/1 to VPF), the Natural Science Foundation of Jiangsu Province (No. BK20190518), the Fundamental Research Funds for the Central Universities (grant no. XUEKEN2022025), and the Jiangxi Branch of China National Tobacco Corporation, China (grant no. 2021.01.010).

AUTHOR CONTRIBUTIONS

WR, ZW, AJ, VPF and SQ conceived the study and designed the experiments; WR, ZY and JW performed the evolution experiment and in vitro and *in planta* assays; BF and SG performed the variant calling analysis; GJ, ZY and JW performed the reverse-genetics experiment; WR, GJ, BF and VPF wrote the manuscript with input from all authors.

COMPETING INTERESTS

The authors declare no competing interests.

ADDITIONAL INFORMATION

Supplementary information The online version contains supplementary material available at https://doi.org/10.1038/s41396-023-01356-6.

Correspondence and requests for materials should be addressed to Waseem Raza, Ville-Petri Friman or Zhong Wei.